

A LIFING PROCEDURE TO PREDICT LIFE FOR SHOT-PEENED CAST COMPONENTS SUBJECTED TO HIGH CYCLE FATIGUE

I. Chantier,¹ V. Bobet-Denier² and F. Hild¹

¹LMT-Cachan, ENS de Cachan / CNRS / Université Paris 6
61 avenue du Président Wilson, 94235 Cachan Cedex, France

²RENAULT Technocentre / Direction de la Recherche / Sce 64230 TCR RUC 4 29
1 rue du Golf, 78288 Guyancourt Cedex, France

ABSTRACT

In many studies on high cycle fatigue, failure occurs at the free surface or close to it. Consequently, the effect of the environment and the surface treatment are of utmost importance. In the case of structures made of spheroidal graphite cast iron, the presence of different kinds of initial flaws within the material explains the scattered fatigue lives. An expression for the cumulative failure probability depending of these initial flaws is derived. For tested suspension arms, this probabilistic approach is used to assess the fatigue lives by taking into account a flaw size distribution, a crack propagation law, the environment and the surface treatment.

INTRODUCTION

Nowadays, the automotive industry is one of the main fields that want to improve the life assessment of safety components made of Spheroidal Graphite (SG) cast iron. Designing components better, faster and cheaper is one of their challenges. In cars, cast components are subjected to High Cycle Fatigue (HCF). On the one hand, the fatigue strength is generally reduced by the presence of initial casting flaws randomly distributed within the material; on the other hand, scattered results are observed in S-N (Woehler) diagrams. The life of cast components depends on two key elements: the state of their surface (as-cast, machined or shot-peened), and the nature of the material microstructure. Lastly, the size and location of flaws can be detrimental to the fatigue resistance and therefore the flaws need to be taken into account by a probability density function.

For any state of the free surface, scattered results of fatigue tests on structures show the need for a probabilistic approach. The cumulative probability of a structure, written for different cycling conditions, depends on an initial flaw size distribution and a microcrack propagation law. The main point of the present

study is the integration of the effects of shot-peening and the environment on the reliability of structures subjected to HCF. The reliability of shot-peened suspension arms is evaluated and compared with experimental data.

MATERIAL

The material studied herein is an SG cast iron essentially ferritic (i.e., containing less than 5% of pearlite). Its composition (wt%) is: C = 3.8, Si = 3.21, Mg = 0.01, S = 0.04, P = 0.007. The main microstructure characteristics are: mean graphite nodule diameter = 17 μm , ferritic grain size = 15/22 μm , mean distance between nodules = 80 μm [1]. For machined samples, the tensile properties are: yield stress = 365 MPa, tensile strength = 500 MPa, elongation = 16%, Young's modulus = 150 GPa.

In the present study, typical casting flaws leading to failure were observed on machined samples designed for HCF. One class of flaws was characterised: microshrinkage cavities within the material (Fig. 1). Their size vary up to 400 μm (i.e., the maximum flaw size a_M). Consequently, these flaws are physically short cracks [2], modelled by penny-shaped cracks whose size is $2a$, and normal is oriented along the direction of the local maximum principal stress σ . The corresponding Stress Intensity Factor (SIF) can be described by $K = Y\sigma\sqrt{a}$ where Y is a geometric dimensionless parameter. Microscopic observations lead us to introduce a flaw size distribution f_0 that describes the flaw population [3]

$$f_0(a) = \frac{a^\alpha (a_M - a)^\beta}{B_{\alpha\beta} a_M^{\alpha+\beta+1}} \quad \text{with} \quad B_{\alpha\beta} = \int_0^1 t^\alpha (t-1)^\beta dt \quad (1)$$

It is assumed that the representative volume V_0 of this material is equal to the gauge volume of tested samples, i.e., 340 mm^3 . Systematic SEM observations allows one the measurement of the flaw sizes observed on fractured surfaces, and therefore the identification of the distribution parameters: $\alpha = 2.3$, $\beta = 18$ and $a_M = 400 \mu\text{m}$. The associated propagation law is a modified Paris' law [3]

$$\frac{da}{dN} = C \Delta K_{eff}^n \quad \text{with} \quad \Delta K_{eff} = \frac{K_{max} g(R) - K_{th}}{K_c - \frac{K_{th}}{g(R)}} \quad (2)$$

and

$$g(R) = \frac{1-R}{1-mR} \quad \text{with} \quad R = \frac{\sigma_{min}}{\sigma_{max}} \quad (3)$$

Under cyclic loading, the initiation period is neglected compared to the stable microcrack propagation period. In HCF, the number of cycles to failure N_F mainly depends on the load ratio R , the threshold SIF K_{th} , the maximum flaw size a_M and the fatigue limit of the largest flaw $S_{th} = K_{th} / Y \sqrt{a_M} g(R)$. The next section introduces the cumulative failure probability on a complex structure.

A PROBABILISTIC APPROACH IN HCF FAILURE

By using the previous analysis, a flaw size distribution f_0 was identified. Under cyclic loading conditions, f_0 evolves with the number of cycles N to become equal to f_N . By considering a representative element Ω_0 of

volume V_0 that contains the initial flaws, the cumulative failure probability P_{F0} is the probability of finding flaws greater than a_c after N cycles

$$P_{F0} = \int_{a_c}^{+\infty} f_N(a) da \quad \text{with} \quad a_c = \left(\frac{K_c}{Y\sigma_{max}} \right)^2 \quad (4)$$

No nucleation of flaws is assumed during the whole load history. By introducing the initial crack size a_{c0} that becomes critical after $N = N_F$ cycles, P_{F0} can be rewritten as

$$P_{F0} = \int_{a_{c0}}^{+\infty} f_0(a) da \quad (5)$$

In other words, more and more critical flaws appear when N_F increases. The framework of the weakest link theory [4] allows one to express the cumulative failure probability P_F of a complex structure Ω of volume V as a function of P_{F0} , by neglecting the flaw interactions

$$P_F = 1 - \exp \frac{1}{V_0} \iiint_{\Omega} \ln(1 - P_{F0}) dV \quad (6)$$

Figure 2 shows the identification of tension tests ($R = 0.1$) on machined samples with the present model [3]. In the next section, the different surface effects are explained in detail.

SURFACE EFFECTS

The surface effects can be summarised as follows: the SIF is a function of the distance of flaws (i.e., cracks) from the free surface, the compressive residual stress field induced by shot-peening slows down the crack propagation rate in the vicinity of the free surface and the environment influences the crack propagation law.

Mechanical layer

As often observed, HCF is typically a surface problem which can be partly explained by mechanical concepts. The size a and the location (depth d from the free surface) of flaws within the material are important to describe the critical flaw for the fatigue life. This surface effect is analysed with the dependence of the maximum SIF K_{max} on the crack size a and the depth d by means of a geometric dimensionless parameter Y [5]

$$K_{max} = Y(a, d) \sigma_{max} \sqrt{a} \quad (7)$$

The closer the defect to the free surfaces, the greater the SIF. The limits are 2 (at the surface) and 1.46 (in the bulk) [5]. By integrating the propagation law with this last expression, the evolution of the flaw size leading to failure with the depth can be described [6]. It follows that the fatigue life is different if the mechanical layer is accounted for or not (Fig. 3).

Propagation law

To introduce the effect of the environment, the distinction between crack propagation in air or in vacuum is made. The crack propagation rate in air is ten times higher than in vacuum for the same SIF range [7]. For

the same flaw size, a crack at the free surface is more critical for the fatigue life than an internal crack subjected to the same stress level.

The first parameter identification concerns the crack propagation law in air. Two methods can be followed:

- first, by considering a constant cumulative failure probability in tension/compression (say 50%), the parameters of the propagation law can be identified [3]: $C/a_M = 5.9 \cdot 10^{-5}$, $K_{th}/K_c = 0.33$, $m = 0.59$, $n = 2.1$ (Fig. 4);
- second, by considering the propagation data for the relevant flaw sizes, the modified Paris' law given by Eqn. 2 is fitted with a constant threshold SIF K_{th} and a constant critical SIF K_c [7]. Similar parameters are found (Fig. 4).

The second parameter identification concerns the crack propagation law in vacuum [7]. In that case, only crack propagation data are available. The following parameters are obtained: $C/a_M = 2.76 \cdot 10^{-3}$, $K_{th}/K_c = 0.163$, $m = 0.59$, $n = 4.23$.

Surface treatment

The shot-peening process allows one to create an initial compressive stress field in the vicinity of the free surface of as-cast components. This stress field induces crack closure, which is beneficial to the fatigue life [8].

By means of X-ray diffraction, the in-plane stresses are measured on samples and suspension arms, which underwent the same double shot-peening treatment. The following results are obtained:

- an initial equibiaxial stress state is obtained whose level is -450 ± 25 MPa for samples and -350 ± 22 MPa for suspension arms;
- after cycling of samples in tension ($R = 0.1$) for a stress level (295 MPa) corresponding to the endurance limit of shot-peened samples when $P_{F0} = 50\%$, the longitudinal residual stress increases by an amount of 200 MPa. Therefore, the stabilised residual stress is -250 ± 20 MPa at the free surface;
- lastly, measurements and Ref. [8] confirm the fact that the compressive stress is present in a surface layer 0.5 mm in depth.

All these effects need to be considered to assess the reliability of structures in HCF. To carry out numerical computations, structures are divided into two entities, viz. a *surface layer* (the shot-peened 'skin') and the remaining *volume*, to distinguish their respective properties (i.e., SIF, propagation law and stabilised initial stress state).

The next section aims at analysing the experiments on suspension arms. In particular, observations of fractured surfaces of arms are carried out to compare them to fractured surfaces of as-cast samples. The reliability of a suspension arm is then evaluated.

APPLICATION TO STRUCTURES

Samples

To analyse the three previous surface effects, computations are carried out on samples 10 mm in diameter. For these calculations, a stabilised compressive stress level of -250 MPa on a 0.5 mm thick surface layer is considered in the case of rotary bending ($R = -1$) with a maximum applied stress σ_F of 350 MPa. The

(positive) influence of shot-peening and the (negative) effect of the mechanical layer on the failure probability are shown in Fig. 3.

Suspension arms

Fatigue tests and observations

Fatigue tests on suspension arms were carried out with a mechanical system that allows one to prescribe biaxial loading along two axes \underline{X} and \underline{Y} in the suspension arm plane, at point E (Fig. 5). To test only the fatigue resistance, its surroundings are simplified: neither its knee joint, nor its bond with the anti-inclination bar are used. Moreover, to have access to a cyclic frequency of 10 Hz, arms are mounted without the elastic bonds. Displacement boundary conditions are prescribed at two points A and B (Fig. 5); apart from a free rotation about the \underline{Z} -axis, the other degrees of freedom are suppressed.

The analysis of fatigue results shows a scatter in an F_X -N diagram. The failures are essentially located along the AB segment, close to the knee joint (Fig. 5). By SEM analysis, microshrinkage cavities are observed as well as degenerated graphite nodules close to the free surface. As a first approximation, we consider that the flaw size distribution is identical in both machined samples and suspension arm because the degenerated graphite nodules are located in the shot-peened layer.

Numerical computations

To assess the predictive capacity of the probabilistic approach, a comparison between fatigue tests carried out on double shot-peened suspension arms and numerical simulations is now performed. A programme, ASTAR, was developed to evaluate the reliability of components subjected to cyclic loading. It allows one to integrate volume and stress field heterogeneity, with the flaw size distribution identified in the first section. The prediction of the local failure probabilities and the global failure probability of a structure is possible. This programme is divided into two parts: ASTAR-SURF for the *surface layer* and ASTAR-VOL for the remaining *volume*.

The post-processor uses an elastic (FE) analysis to determine the stress field in structures: at each integration point, the equivalent stress is computed (e.g., maximum principal stress). To this equivalent stress corresponds an initial flaw size a_{c0} for a given number of cycles of failure N_F . This flaw size is computed by integration of Eqn. 2 through a Newton method. The failure probability P_{Fj} of an element j in a structure can be calculated: P_{Fj} depends on the element volume V_j , the number n_g of integration points for this element and the weight w_i associated with each integration point

$$\ln(1 - P_{Fj}) = \frac{V_j}{V_0} \sum_{i=1}^{n_g} \ln(1 - P_{Fi}) w_i \quad (8)$$

where P_{Fi} denotes the cumulative failure probability at point i , evaluated by using Eqn. 5. The failure probability P_F^k of one entity of the structure (viz. surface layer or remaining volume) is then computed

$$P_F^k = 1 - \exp \left[\sum_{j=1}^{n_k} \ln(1 - P_{Fj}) \right] \quad (9)$$

where n_k is the number of elements of one part of whole structure and k stands for either the *surface layer* or the remaining *volume*. Lastly, the failure probability P_F of the whole structure is computed as follows

$$P_F = 1 - (1 - P_F^{Surf})^{\frac{V_{Surf}}{V}} \times (1 - P_F^{Vol})^{\frac{V_{Vol}}{V}} \quad \text{with} \quad V = V_{Surf} + V_{Vol}. \quad (10)$$

Results

For a given flaw size distribution, constant cumulative failure probabilities 10% and 90% are plotted in Fig. 6 for $R = 0.1$. The predictions are in good agreement with experimental fatigue data. Since the volume of the *surface layer* is less than that of the remaining *volume* and the shot-peening process induces no failure in the surface layer ($P_F^{Surf} = 0$), the crack propagation law in vacuum governs the cumulative failure probabilities.

Furthermore, by inspection of the contours of local cumulative failure probabilities, the most likely sites of failure correspond to those observed experimentally (Fig. 5). These results show that the flaw location with respect to the stress field is of utmost importance: to be critical a defect needs to be subjected to a minimum stress level (such that $\Delta K_{eff} \geq 0$).

CONCLUSIONS

This study shows the need for a probabilistic approach to assess the fatigue life of SG cast iron structures. To be predictive, the approach needs to account for three different surface effects:

- a mechanical effect leading to a dependence of the stress intensity factor on the depth from the free surface of the considered crack;
- an environmental effect requiring to consider crack propagation laws in air (in the vicinity of the free surface) and in vacuum (in the bulk of the material);
- the surface treatment (i.e., as-cast, shot-peened or machined) and the corresponding stabilised residual stress field induced by the whole process.

A post-processor, which integrates the previous effects, was written to analyse complex structures. In particular, the stabilised residual stresses are measured and considered as an input of the programme. By using the present probabilistic approach, the flaw size distribution and crack propagation parameters are first identified on samples and then used to predict the reliability of suspension arms. A good agreement between experimental data and numerical predictions is obtained for suspension arms. It is shown that the reliability of suspension arms is governed by the bulk properties since no failure occurs in the surface layer thanks to the shot-peening treatment.

Furthermore, this lifing procedure gives also some guidelines to decide whether to reject (NDE)-controlled cast components. To be critical, a defect needs to be subjected to a minimum stress level (such that $\Delta K_{eff} \geq 0$). Therefore, different defect locations lead to different critical defect sizes.

ACKNOWLEDGEMENTS

This work was supported by Renault through contract CNRS / 1996 / 014 (H5.24.12) with LMT-Cachan.

REFERENCES

1. Clément, P., Angeli, J.-P. and Pineau, A. (1984) *Fatigue Eng. Mater. Struct.* **7**, pp. 251-265.
2. Miller, K.J. (1997). In: *Fatigue and Fracture Mechanics*, **ASTM STP 1296**, pp. 931-939, Piascik, R.S., Newman, J.C. and Dowling, N.E. (Eds), ASTM, Philadelphia.
3. Yaacoub Agha, H., Béranger, A.-S., Billardon, R. and Hild, F. (1998) *Fatigue Fract. Engng. Mater. Struct.* **21**, pp. 287-296.
4. Freudenthal, A.M. (1968). In: *Fracture 2*, pp. 591-619, Liebowitz, H. (Ed.), Academic Press, New York.
5. Murakami, Y. (1981). In: *Stress Intensity Factors Handbook*, Pergamon Press, Oxford.
6. Chantier, I., Bobet, V., Billardon, R. and Hild, F. (2000) *Fatigue Fract. Engng. Mater. Struct.* (in press).
7. Nadot, Y., Ranganathan, N., Mendez, J. and Béranger, A.-S. (1997) *Scripta Materialia* **37**, pp. 549-553.
8. 12^e Conférence Nationale (1991). *Le grenailage de Précontrainte, Mécanique et Procédés*, Publications du CETIM, Senlis (in French).

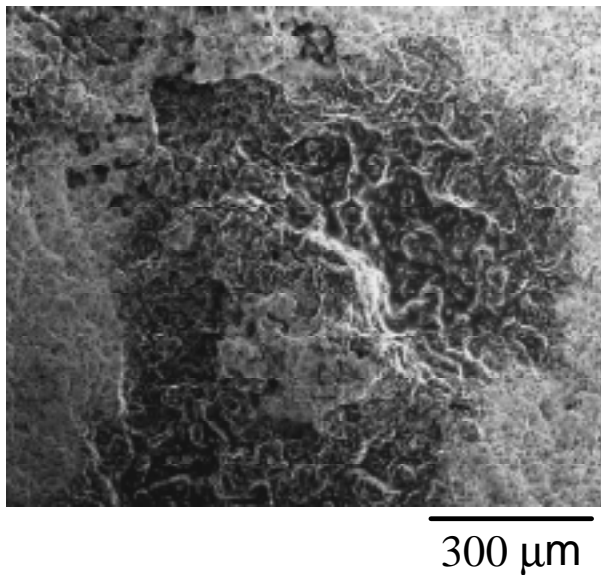


Figure 1: Microshrinkage cavity observed in a suspension arm

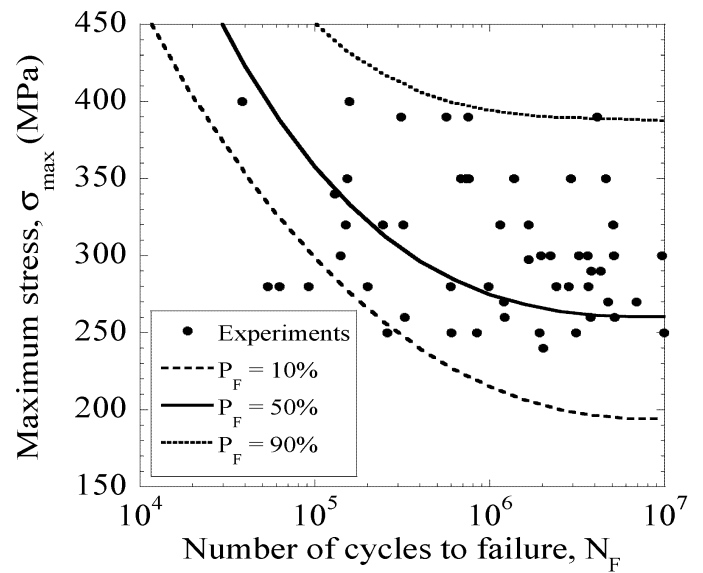


Figure 2: Identified failure probabilities compared with experiments for $R = 0.1$ [3]

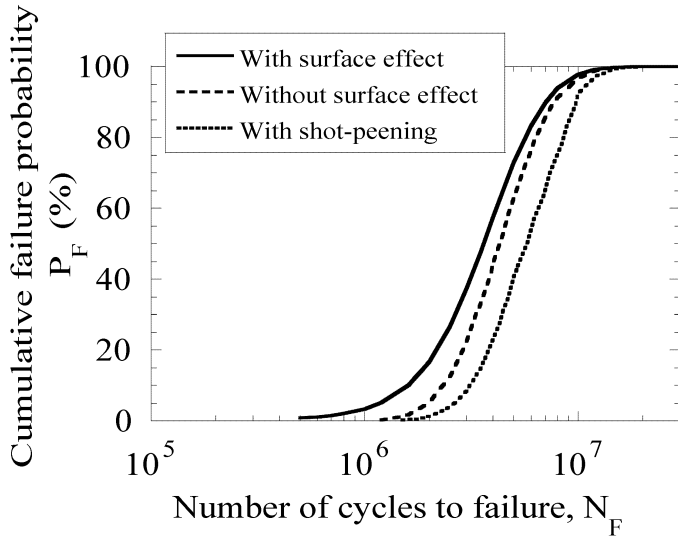


Figure 3: Effect of the mechanical layer and shot-peening on the failure probability ($\phi = 10$ mm, $\sigma_{\text{shot-peening}} = -250$ MPa and $\sigma_F = 350$ MPa)

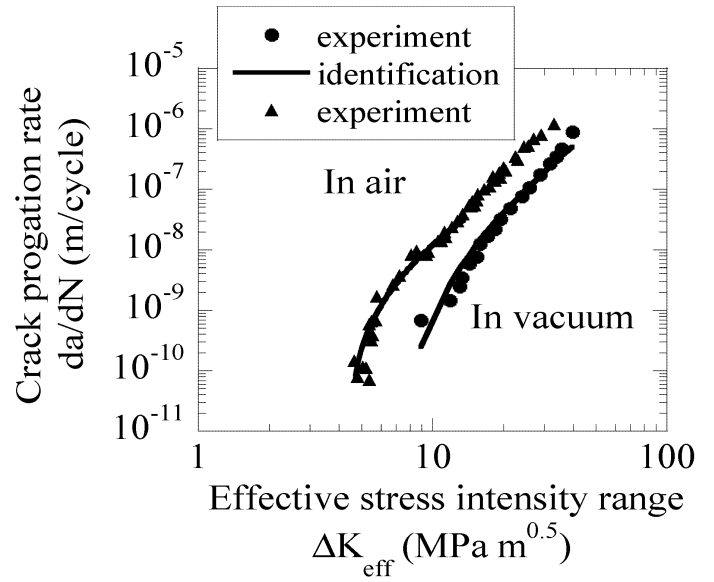


Figure 4: Experimental and identified crack propagation laws in air and in vacuum

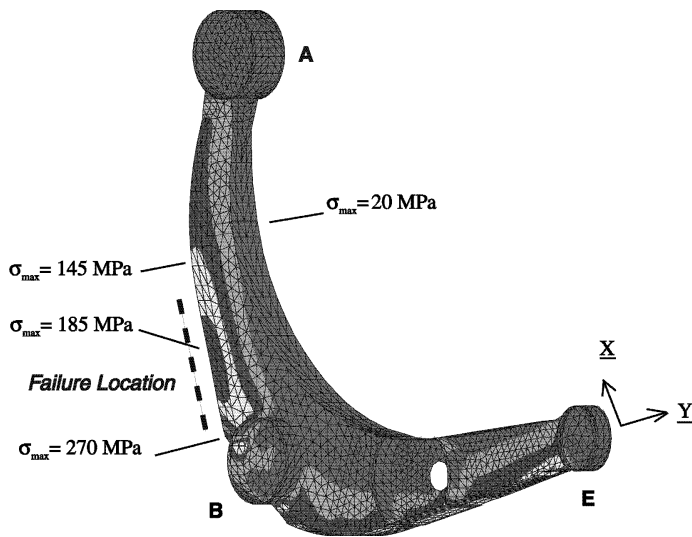


Figure 5: Contours of maximum principal stress and failure location on suspension arms observed in tests and numerical simulations

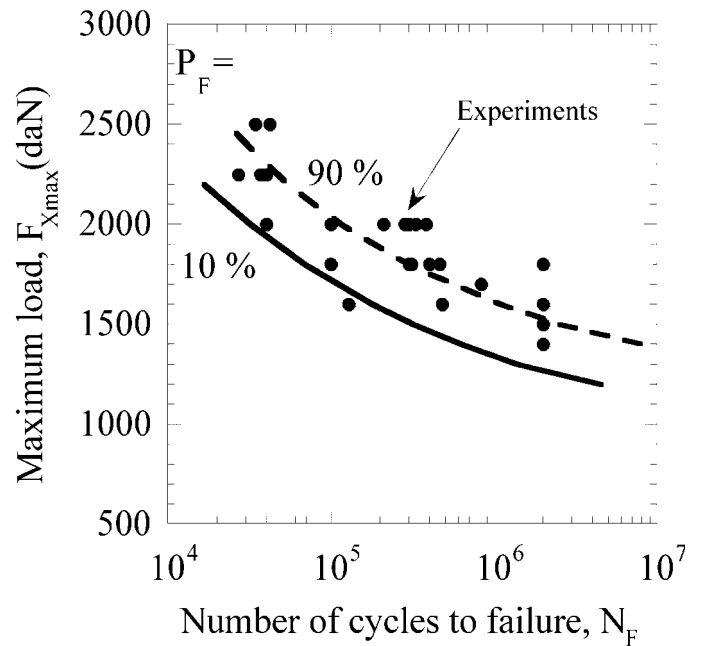


Figure 6: Predicted cumulative failure probabilities and experiments on suspension arms ($R = 0.1$)